RSC Advances

PAPER

View Article Online
View Journal | View Issue

Cite this: *RSC Adv.*, 2025, **15**, 27652

A carrier-free therapeutic eutectogel: construction, physical properties, and anti-bacterial ability

Jing Yuan, [ab] Zhuoni Liu,[c] Tianxiang Yin *[c] and Shengxi Meng*[a]

Received 25th May 2025
Accepted 21st July 2025

DOI: 10.1039/d5ra03681j

rsc.li/rsc-advances

Eutectogels have emerged as promising materials with broad application potential. Herein, therapeutic deep eutectic solvents (THEDESs) based on the active pharmaceutical ingredients oxymatrine and lauric acid were developed. The physical properties, *i.e.*, density, refractive index, surface tension, and viscosity, of the THEDESs were measured. Among these investigated THEDESs, THEDES (3 : 7) has been shown to self-aggregate into a gel in water. The rheological behavior, microscopic structure of the eutectogel, and the gelation mechanism were further explored. Furthermore, THEDES (3 : 7) can enhance the solubility and stability of curcumin effectively. The eutectogel (with and without curcumin) possessed good antioxidant and anti-*P. acnes* activity. To summarize, a simple method based on the self-assembly of THEDES in water was proposed to construct a therapeutic eutectogel, which could potentially be extended as a generalized strategy.

1. Introduction

Acne, commonly known as pimples, is a common skin disease that mainly affects hair follicles and sebaceous gland units, leading to chronic inflammation. The causes of acne are complex, mainly including abnormal androgen levels, vigorous sebum secretion, and immune inflammatory response caused by *P. acnes*. Acne mainly appears in areas with abundant sebaceous glands such as the face, neck, chest, and back, which may damage patients' physical and mental health. Therefore, more and more progress on the treatment of acne has been made in recent decades, where, for instance, topical medication with peroxybenzoyl and azelaic acid has been widely adopted for acne treatment. Recently, fatty acids (FAs), especially capric acid and lauric acid, have been shown to display high activity in inhibiting *P. acne*-induced inflammatory responses by suppressing MAPK phosphorylation and NF-kB activation.[1,2] They can serve as good candidates for acne treatment. However, due to their poor solubility, further clinical applications have been hindered and the construction of complex carriers, such as micelles or liposomes, is required for these FAs.[3–5]

Deep eutectic solvents (DESs) are usually prepared by mixing a hydrogen-bond donor (HBD) component and a hydrogen-bond acceptor (HBA) in suitable ratios.[6,7] They offer the advantages of generating no waste during preparation and being easily designable and are generally considered a new generation of ecologically benign, green, and sustainable solvents.[8,9] Of note, a new type of DES termed therapeutic deep eutectic solvents (THEDESs) have been proposed and drawn much attention, where an active pharmaceutical ingredient (API) was used to construct the DES. THEDESs have displayed great advantages in increasing the solubility, stability, permeation ability and bioactivity of APIs.[10–12] This new strategy has been applied to develop saturated fatty acid-based DESs, which exhibited good antimicrobial properties against a broad spectrum of microorganisms.[13,14]

According to traditional Chinese medicine, a series of active pharmaceutical ingredients (APIs) derived from natural plants, such as curcumin (Scheme 1a)[15–17] and oxymatrine[18,19] (Scheme 1b), have been proven to be highly efficacious in treating skin diseases. It has been reported that deep eutectic solvents prepared from oxymatrine and a fatty acid can be used as a new type of permeation enhancer.[20] Moreover, we have recently shown that some lauric acid-based DESs can form a gel with the addition of water,[21,22] which would be favorable for further clinical applications. Therefore, in this work, oxymatrine is used in combination with lauric acid construct therapeutic DESs (THEDESs). The phase behavior and physical properties have been studied. Moreover, a eutectogel based on a THEDES was developed, and the corresponding macroscopic and microscopic properties were investigated. In addition, the THEDES efficiently enhanced solubility and stability of curcumin. The anti-*P. acnes* activity of the THEDES gel in the absence and presence of curcumin was studied. To sum up, a carrier-free eutectogel system has been constructed, demonstrating great potential for acne treatment.

[a]*Shanghai Sixth People's Hospital Affiliated to Shanghai Jiao Tong University School of Medicine, Shanghai 200233, China. E-mail: mengsx163@163.com*

[b]*Shanghai Sixth People's Hospital East Affiliated to Shanghai University of Medicine & Health Sciences, Shanghai 201306, China*

[c]*School of Chemistry and Molecular Engineering, East China University of Science and Technology, Shanghai 200237, China. E-mail: yintx@ecust.edu.cn*

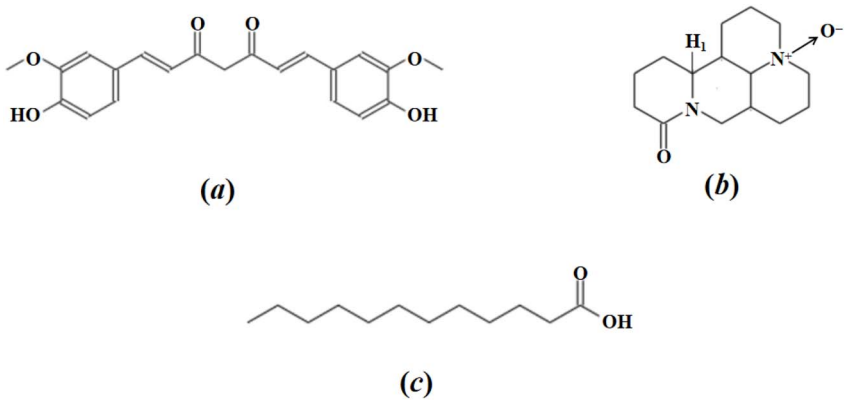

Scheme 1 Chemical structures of (a) curcumin, (b) oxymatrine, and (c) lauric acid.

2. Experimental section

2.1. Materials

Oxymatrine (OMT, 16837-52-8, >98%) and lauric acid (LA, 143-07-7, >99%) were purchased from Adamas. 2,2-Diphenyl-1-picrylhydrazyl (DPPH, 1898-66-4, 96%) and curcumin (Cur, 458-37-7, 98%) were supplied by Maclin. Phosphate-buffered saline (PBS, pH = 7.4, 0.01 M), ethanol (64-17-5, 99.5%), and LB (Luria-Bertani) liquid medium were provided by Aladdin. No further purification was carried out on any of the chemicals. Water used herein was prepared using a commercial ultra-pure water system (model: DZG-303A, supplied by Leading Water Treatment Co. Ltd, Shanghai).

2.2. Preparation and physical properties of DESs

Oxymatrine and lauric acid mixtures at various molar ratios were precisely weighed and stirred at 60 °C for 1 h. Then, the samples were slowly cooled to room temperature (298 K). The samples that still appeared as homogeneous liquids were chosen as THEDESs.

^{1}H NMR spectra of THEDESs, oxymatrine, and lauric acid were obtained using a Bruker Avance 500 spectrometer with $CDCl_3$ as the solvent at 298 K. Fourier transform infrared (FT-IR) spectra of these samples were also collected by using a Nicolet 6700 FT-IR spectrometer (ThermoFisher Scientific, USA) *via* the ATR method in the wavenumber range from 400 cm^{-1} to 4000 cm^{-1}. Thermograms from differential scanning calorimetry measurements were obtained for these samples in the temperature range from −40 °C to 200 °C with a scan rate of 10 °C min^{-1} using DSC 2910 apparatus (TA Instruments, USA).

Physical properties like density, viscosity, refractive index and surface tension of THEDESs were measured in the temperature range from 298.15 K to 348.15 K. Detailed descriptions of the setup and procedure can be found in our previous publications.[23–25]

2.3. Properties of eutectogels

Phase behaviors of THEDES–water mixtures were determined by directly observing the fluidity of samples during the cooling process from 90 °C to 25 °C.

Microscopic structures of eutectogels were investigated *via* scanning electron microscopy (SEM) using an FEI Quanta 450 SEM (FEI, USA) equipped with an Everhart Thornley detector. The sample was frozen and sputter-coated with platinum before measurements.

Rheological measurements, *i.e.*, viscosity measurements, strain sweep experiments, and frequency sweep tests, were performed in a rotary rheometer (Anton Paar MCR302) using parallel-plate geometry (50 mm diameter, 1 mm gap) at 298.15 K. Details of the measurement procedure can be found in previous reports.[21,22]

2.4. Solubility and stability of curcumin in THEDES

A mixture of an excess amount of curcumin and 10 mL of THEDES was prepared and further vigorous stirring was performed on the mixture at 298.15 K for 72 h. Thereafter, the mixture was centrifuged at 10 000*g* for 30 min to remove any possible undissolved curcumin. Samples were prepared by mixing a certain amount of supernatant and ethanol, and they were further analyzed using a UV-Vis spectrometer (UV-2450, Shimadzu) to determine the solubility of curcumin.

0.01 mg mL^{-1} curcumin solutions in THEDES or water (including 10% ethanol) were prepared and then either irradiated at 254 nm or heated to 50 °C. The absorption spectra of curcumin were recorded for 6 h at 30 minute intervals to assess its stability.

The stability of curcumin was also evaluated based on the radical scavenging activity using the DPPH method. Briefly, a mixture of 20 mg mL^{-1} curcumin in THEDES was prepared first. Thereafter, it was mixed with ethanol to produce an alcoholic solution of the (curcumin + THEDES) mixture with different compositions (this mixture is termed as sample). 2 mL of 0.2 mM DPPH alcohol solution was thus mixed with an equal volume of sample, and the absorbance of the mixture at 515 nm was recorded after 30 min using a UV-Vis spectrometer, and this was denoted as A_{sample}. Moreover, UV-Vis spectra of (ethanol + sample) and (ethanol + DPPH solution) mixtures were obtained, and the absorbance at 515 nm was recorded as A_{blank} and $A_{control}$, respectively. The scavenging activity was then estimated from the following expression:

$$\text{Activity}(\%) = \left(1 - \frac{A_{\text{sample}} - A_{\text{blank}}}{A_{\text{control}}}\right) \times 100\% \quad (1)$$

2.5. Molecular dynamics simulations

Molecular dynamics (MD) simulations were conducted using Materials Studio (MS) software, and all calculations were performed using Materials Studio 2020. A 33 × 33 × 33 Å simulation box containing a total of 100 DES molecular units was constructed, and then curcumin molecules at a molar fraction of 5% were added to establish the solution model. The simulation steps are as follows: (i) Materials Studio is used to construct the simulation box, after which the annealing algorithm is used to minimize the energy with the temperature being set from 300–1000 K. 15 cycles were carried out, and structure optimization was performed in each cycle; (ii) the frame with the smallest energy in the model was selected as the NPT systematic conditions of 298 K and 1 bar; then a simulation step length of 1 fs and a simulation step count of 1 000 000 steps was used, sampling every 5000 steps, giving a total duration of the dynamics simulation of 1 ns; (iii) cohesive energy density calculations were carried out after the dynamics simulation. All simulation processes used the COMPASS force field, the Andersen method[26] was used to control temperature, and the Berendsen method[27] was used to control pressure. Finally, the radial distribution function (RDF) of the system was calculated.

2.6. Anti-bacterial activity

Anti-bacterial activity assays were performed by using a similar procedure as reported previously.[22] Briefly, a *P. acnes* solution with a concentration of 10^6 CFU (colony forming units) mL^{-1} was prepared first and 100 μL of this solution was spread uniformly on a Petri dish with LB solid medium, which was punched with a 10 mm hole punch. Thereafter, 40 μL of sterilized sample was taken and added into the holes. The Petri dish was placed in an incubator for 72 h with a constant temperature of 37 °C. Finally, images of the Petri dish were captured, and the corresponding inhibition zone size was determined.

3. Results and discussion

3.1. Phase behavior and physical properties of THEDESs

A series of oxymatrine and lauric acid mixtures with molar ratios of 1 : 9, 2 : 8, 3 : 7, 4 : 6, 5 : 5, 6 : 4, 7 : 3, 8 : 2 and 9 : 1 was prepared and heated to 60 °C. After these mixtures were cooled to 298 K, only a few of them retained their homogenous liquid state, *i.e.*, mixtures with molar ratios of 3 : 7, 4 : 6, and 5 : 5, as displayed in Fig. 1.

Physical properties are of significant importance for both theoretical understanding and practical applications of THEDESs. For instance, refractive index is a significant optical property that reflects the change in the speed of light when it moves from one medium to another; density, especially the influence of temperature on density, describing the tendency of a fluid to expand when heated or cooled, is important for industrial operations; surface tension is an important property that characterizes the liquid–air interface; and viscosity, which describes the mobility and flow resistance of solvents, is a crucial property when designing and optimizing various industrial processes. Therefore, we measured the refractive index, surface tension, density and viscosity of these THEDESs in the temperature range between 298.15 K and 348.15 K, as shown in Fig. S1 in the SI. The density and refractive index values of THEDESs are slightly higher than those of water, while the surface tension values of THEDESs are lower. In addition, the viscosity values of THEDESs are significantly high, which may be due to the extensive H-bonding network. Generally, the nature of both the HBD and HBA, the molar ratio of the HBD to HBA, and temperature may all change the physical properties of DESs.[28] The density, refractive index, and surface tension values of all investigated THEDESs decrease linearly with increasing temperature, as is commonly observed in DESs, which generally results from a decline in H-bonding strength with increasing temperature. The change of viscosity with temperature can be modelled using an Arrhenius-type equation:

$$\eta = \eta_0 \exp\left(-\frac{E_a}{RT}\right) \quad (2)$$

where E_a refers to the activation energy. The activation energies are determined to be 55.3, 63.2, and 68.2 kJ mol^{-1} for THEDESs with molar ratios of 3 : 7, 4 : 6 and 5 : 5, respectively. A higher activation energy means higher viscosity, coinciding well with the experimental results. Furthermore, all these explored physical properties displayed a tendency to decline with an increase in the HBD component. It has been reported that an increase in molecular weight would cause an increase in physical properties like density, viscosity, *etc.*[29] As the molecular weight of oxymatrine is higher than that of lauric acid, an increase in the HBD (lauric acid) component may result in a decline in the molecular weight of the THEDES, which would reduce the explored physical properties.

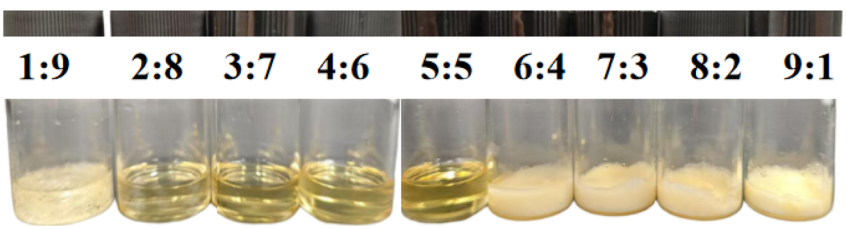

Fig. 1 Images of a series of oxymatrine and lauric acid mixtures at 298 K.

Moreover, surface tension has been proposed to relate to refractive index or viscosity based on the Papazian equation: $\gamma = c\frac{n^2-1}{2n^2+1} + d$ or $\ln\gamma = A + B\ln\eta$, according to Pelofsky and Murkerjee, with A, B, c and d being adjustable parameters.[30,31] Therefore, plots of surface tension against $n^2 - 1/2n^2 + 1$ and plots of $\ln\eta$ against $\ln\gamma$ are shown in Fig. S2 in the SI, where linear relationships are clearly shown.

3.2. THEDES as a solubility and stability enhancer of curcumin

THEDESs were mixed with water at a series of water ratios from 0% to 100% at 298 K. It was found that only the THEDES with an oxymatrine and lauric acid molar ratio of 3 : 7 displayed obvious gelation behavior. Considering the similarity of matrine with oxymatrine studied herein, it is not surprising that both matrine- and oxymatrine-based DESs with a molar ratio of 3 : 7 can self-aggregate into gels in water. Therefore, this THEDES, *i.e.*, the sample with a molar ratio of oxymatrine to lauric acid of 3 : 7, was chosen for the following studies.

The formation of THEDES (3 : 7) was further evaluated by ^{1}H NMR, FT-IR and DSC measurements, as shown in Fig. 2. From the ^{1}H NMR spectrum (Fig. 2a), the ratio of the peak areas at δ = 0.85 (–CH_3 from lauric acid) and δ = 4.66 (H_1 from oxymatrine; see Scheme 1b) was calculated to be 2.35, corresponding to the molar ratio of oxymatrine to lauric acid being 3 : 7. FT-IR spectra are displayed in Fig. 2b, where the stretching peak of C=O from lauric acid at 1702 cm^{-1} declines and shows an obvious shift toward a higher wavenumber at 1720 cm^{-1}, accompanying the formation of the THEDES. Meanwhile, the vibration of N^+–O^- at 2290 cm^{-1} is not found in the THEDES, while the stretching vibration of C=O in oxymatrine at 1610 cm^{-1} shows slight movement toward a lower wavenumber. Therefore, the formation of the THEDES can be reasonably ascribed to the interaction between the –COOH group from lauric acid and N^+–O^- from oxymatrine. Moreover, the characteristics of a low melting temperature (−10 °C) and a single peak for THEDES are both presented in the thermograms from DSC measurements, as displayed in Fig. 2c.

It has been extensively proven that DESs can enhance the solubility and stability of poorly soluble APIs.[32–35] Therefore, the solubility and stability of an important API from traditional Chinese medicine, curcumin, were evaluated. Curcumin is a widely used natural polyphenol that is usually extracted from the *Curcuma longa* species, which has been used to treat various skin diseases due to its high antioxidant and anti-inflammatory activities.[15] Moreover, combining curcumin with lauric acid resulted in a synergistic effect against *P. acnes*.[17] However, the extremely poor water solubility (0.6 μg mL^{-1})[36] and bioavailability, as well as low stability, of curcumin have greatly hindered its clinic applications. Recently, the use of (deep) eutectic solvents, such as choline chloride + levulinic acid,[37]

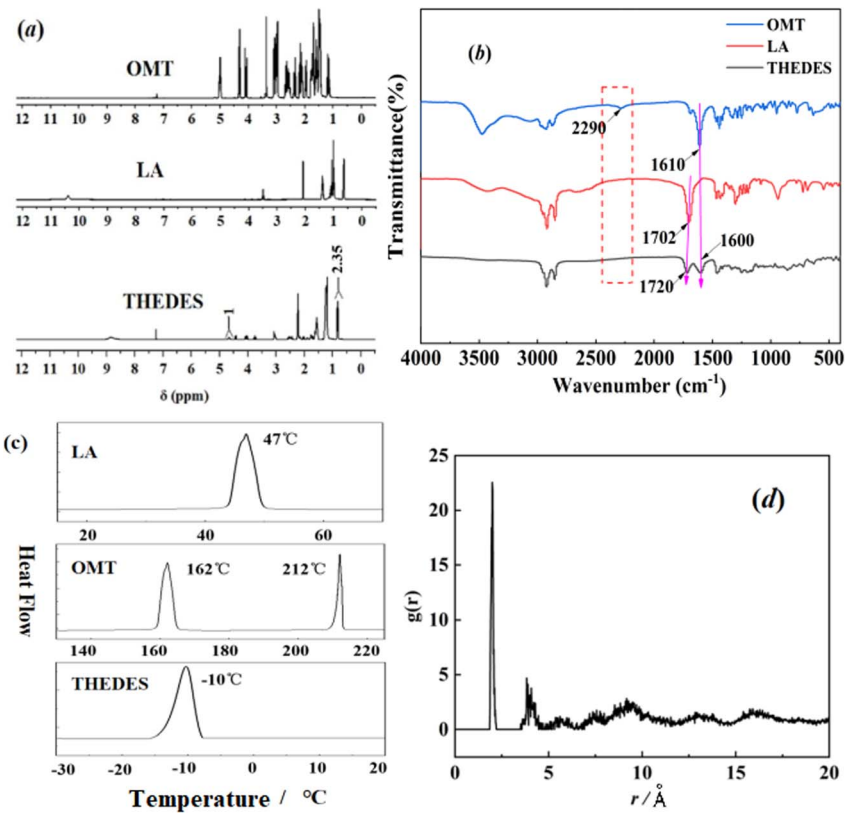

Fig. 2 (a) ^{1}H NMR spectra, (b) FT-IR spectra and (c) thermograms from DSC measurements for oxymatrine (OMT), lauric acid (LA) and the THEDES. (d) RDF analysis of the curcumin-THEDES system.

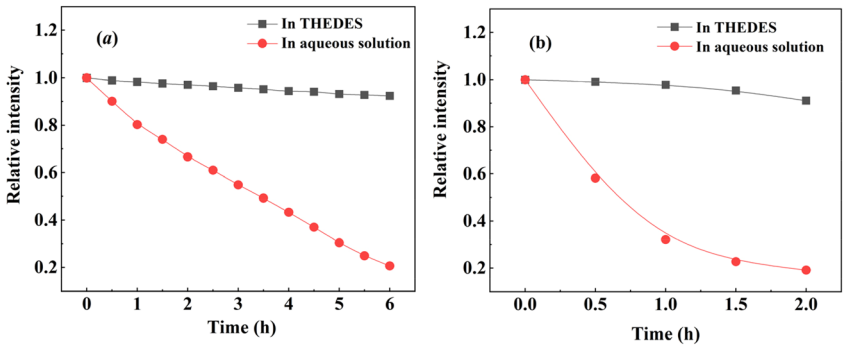

Fig. 3 Variations of the relative intensity of curcumin absorbance in the THEDES and in aqueous solution (with 10% ethanol) over time: (a) under 254 nm irradiation and (b) at 50 °C.

choline chloride + glycerol,[38] and matrine + caprylic acid,[23] has been suggested for the utilization of curcumin.

The calibration curve for curcumin in ethanol was determined previously,[22] and it was used herein to calculate the solubility of curcumin. It should be mentioned that the UV-Vis spectra of the THEDES in ethanol in the absence and presence of curcumin were obtained, and a negligible influence from the THEDES on the adsorption of curcumin in ethanol was found. The obtained solubility of curcumin in presented THEDES was 25.0 mg mL^{-1}, which is 40 000-fold higher than in water. To deepen our understanding of the interaction patterns of curcumin molecules, RDF was applied to analyze the intermolecular interactions. Generally, the larger the radial distance (horizontal coordinate), the weaker the intermolecular interactions are, and *vice versa*. The type and magnitude of interactions between particles can be inferred from the positions and heights of the peaks. Fig. 2d displays RDF analysis of curcumin molecules in THEDES. It can be observed from the figure that the main peaks are present at distances of 1.95 Å and 3.96 Å, which suggests that curcumin may exhibit stronger intermolecular interactions through hydrogen bonding and van der Waals forces. Furthermore, the stability of curcumin in the THEDES was evaluated. A solution of curcumin in the THEDES at a concentration of 0.1 mM was irradiated at 254 nm, and the values of absorbance relating to the maximal absorption wavelength A_{max} were recorded at certain intervals for 6 h. The relative intensity was defined as the ratio of A_{max} to that at the initial time, $A_{max,0}$, (*i.e.*, relative intensity $= A_{max}/A_{max,0}$) and this is plotted in Fig. 3a. For comparison, the result in aqueous solution (in the presence of 10% ethanol to increase the solubility) was also reported and is displayed in Fig. 3a. It can be seen that curcumin displayed much higher stability in the THEDES. Moreover, the stability of curcumin in the THEDES and in aqueous solution (in the presence of 10% ethanol) at a higher temperature of 50 °C was also investigated. The results presented in Fig. 3b further suggest the high stability of curcumin in the THEDES.

3.3. Construction and bioactivity of a eutectogel

Supramolecular gels based on the self-assembly of low-molecular-weight gelators (LMWGs) have been extensively applied in fields like drug delivery, molecular biomaterials, environmental remediation, chemical reactions, *etc.*[39,40] Till now, two types of eutectogel have been reported. First, several LMWGs, like amino acids,[41] alkylaminoamide,[42] and 1,3:2,4-dibenzylidene-D-sorbitol (DBS),[43] have been reported to self-assemble in a DES to form a eutectogel. Another type of eutectogel has been proposed recently, where DESs were applied as gelators to self-assemble into a eutectogel in water, for instance,

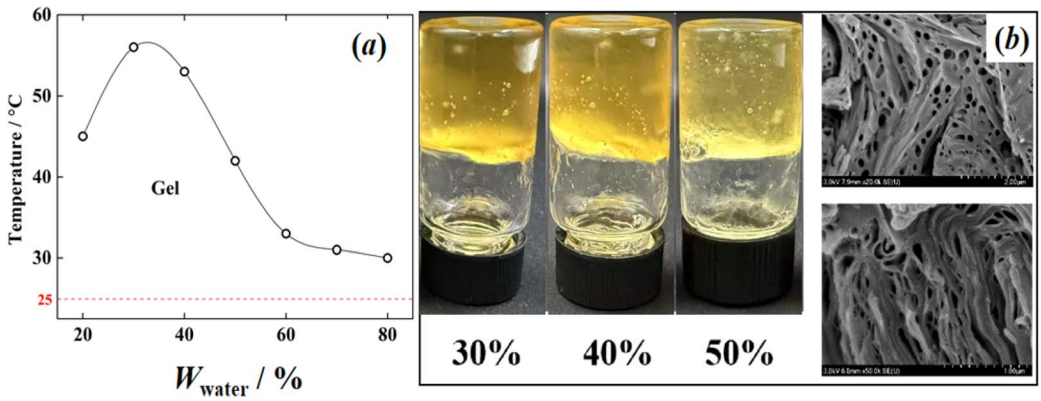

Fig. 4 (a) The temperature–mass fraction phase diagram of THEDES + water; (b) physical photos of eutectogels (in the presence of curcumin) with various water mass fractions (30%, 40% and 50%) and SEM images of a eutectogel (mass fraction of water: 30%) at 25 °C.

lidocaine + lauric acid,[21] decanoic acid + dodecanoate sodium,[44] and matrine + lauric acid.[22]

The temperature–mass fraction phase diagram of a binary THEDES + water system was determined above 25 °C and is shown in Fig. 4a, where a gel phase can be obviously observed when the water mass fraction ranged from 30% to 50%. Photos of eutectogels (in the presence of curcumin) with water mass fractions of 30%, 40% and 50% were captured, which are displayed in Fig. 4b together with SEM images of the eutectogel with 30% water (mass fraction). The 3D network of the eutectogel is clearly indicated from the SEM images. Similar to a eutectogel formed from matrine + lauric acid,[22] hydrophobic interactions between lauric acid tails played an important role in the gelation process, while oxymatrine may act as a solubility enhancer.

The rheological behavior is one of the most important properties when using gels. Therefore, the rheological behaviors of eutectogels formed from this THEDES were investigated. Flow measurements of eutectogels formed from THEDES + water with water mass fractions of 30%, 40% and 50% were carried out, and the variation of viscosity with shear rate is shown in Fig. S3 in the SI, where all eutectogels display typical non-Newtonian fluid behavior, suggesting a strong shear-thinning phenomenon. Furthermore, strain and frequency sweep experiments were performed, and the results are displayed in Fig. 5a and b. It can be seen from Fig. 5a that higher elastic modulus (G') values are seen than those of viscous modulus (G'') in the linear viscoelastic region (LVR). Furthermore, as shown in Fig. 5b, the values of G' and G'' are independent of frequency at a low strain of 0.5%. All these results shown in Fig. 5a and b suggest the formation of strong gels, which is also reflected in the small values of dynamic loss tangent ($\tan\delta = G''/G'$), which were 0.29, 0.23, and 0.21 for eutectogels with water mass fractions of 30%, 40% and 50%, respectively.

Moreover, the thixotropic behaviors of the eutectogels were also investigated based on rheological measurements. The results for the eutectogel with a water mass fraction of 30% are shown in Fig. 5c as an example. At low strain, the eutectogel presents in a quasi-solid state with a high G' value. However, a sharp decline of G' is observed when a large strain is applied, and the eutectogel behaves like a liquid. The eutectogel recovers to a quasi-solid state when the strain is quickly changed to low strain. These phenomena clearly suggested the injectable properties of the presented eutectogel, which would be more favorable for its further applications.

Antioxidant activity is one of the most important forms of bioactivity of curcumin. The antioxidant ability of the THEDES and curcumin in THEDES solution are evaluated using the DPPH radical scavenging assay. The results are presented in Fig. 6a. It can be seen that the THEDES solution of curcumin displayed obvious concentration-dependent behavior. Moreover, at the same concentration (2 mg mL^{-1}), the THEDES itself displays much weaker antioxidant activity (7.4%) as compared to the THEDES solution of curcumin (63.8%), which can be ascribed to the higher inherent antioxidant activity of curcumin and high stability of curcumin in the presented THEDES. Furthermore, the scavenging activities of a newly prepared curcumin-containing eutectogel sample (mass fraction of curcumin: 2 mg g^{-1}) and a sample after storage for 3 weeks were

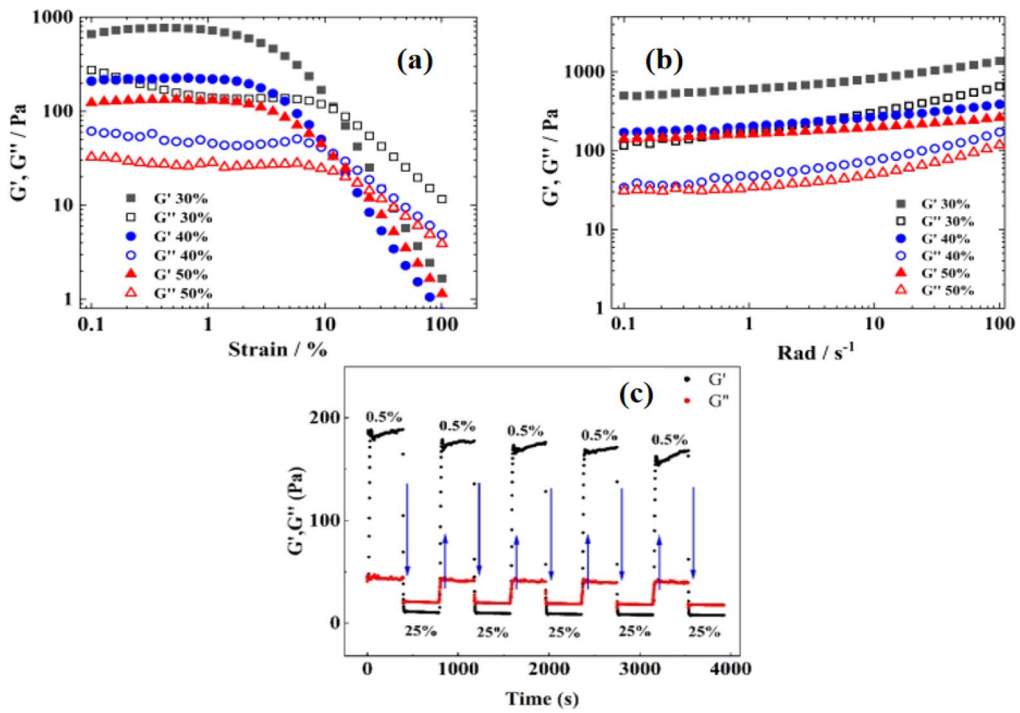

Fig. 5 (a) Strain sweep ($\omega = 1$ Hz) and (b) frequency sweep ($\gamma = 0.5\%$) measurements for eutectogels; and (c) thixotropic results from rheological measurements for the eutectogel with a water mass fraction of 40%.

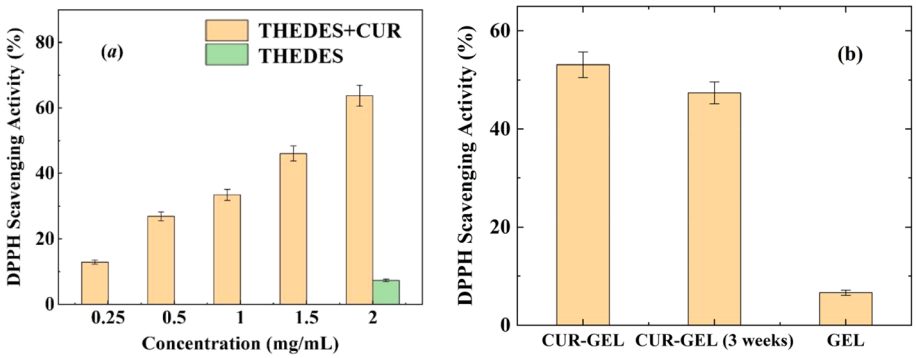

Fig. 6 (a) Variation of the scavenging activity with concentration for THEDES solutions of curcumin; and (b) the change in scavenging activity of a curcumin-containing eutectogel after being stored for 3 weeks.

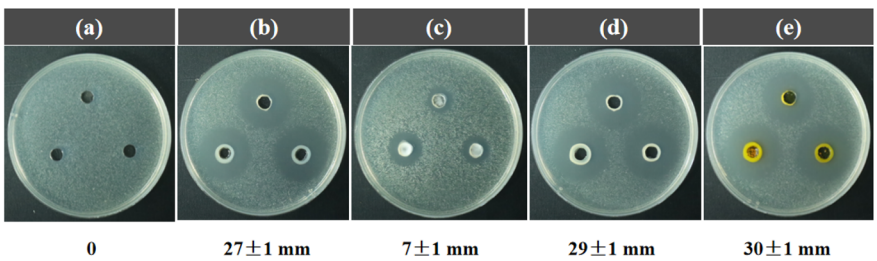

Fig. 7 Anti-*P. acnes* activities of (a) DMSO, (b) 5% BPO gel, (c) 15% azelaic acid gel, (d) the eutectogel, and (e) the eutectogel with curcumin.

determined and compared in Fig. 6b. It can be seen that the eutectogel possesses high antioxidant ability, and 90% of curcumin remained unchanged during this period, highlighting the high stability of curcumin in the eutectogel.

It was mentioned above that both lauric acid and curcumin possess anti-*P. acnes* properties, while oxymatrine also shows great pharmacodynamics towards various skin diseases. Therefore, an evaluation of the anti-*P. acnes* ability of the eutectogel was performed and it was compared to commercial anti-*P. acnes* drugs. The results are presented in Fig. 7, where 5% BPO (benzoyl peroxide) gel and 15% azelaic acid gel obtained from a local pharmacy were used for comparison. The diameters of inhibition zones are summarized and listed in Fig. 7.

It can be seen from the above explorations that the presented eutectogel (both in the presence and absence of curcumin) displayed better anti-*P. acnes* bioactivity than commonly used commercial BPO and azelaic acid gels, making the prepared eutectogel a potential candidate for acne treatment. The addition of curcumin slightly increased the anti-*P. acnes* activity of the prepared eutectogel. Therefore, a carrier-free therapeutic eutectogel based on an oxymatrine + lauric acid THEDES was constructed and displayed great potential for application in acne treatment.

4. Conclusions

In this study, therapeutic deep eutectic solvents based on the active pharmaceutical ingredients oxymatrine and lauric acid were developed. Physical properties, like density and viscosity, of THEDESs with oxymatrine to lauric acid molar ratios of 3 : 7, 4 : 6, and 5 : 5 were measured. Both density and viscosity decline with temperature. Moreover, the prepared THEDES (3 : 7) can self-aggregate into a gel in water, which was further explored *via* rheological experiments and SEM measurements. Furthermore, THEDES (3 : 7) efficiently enhanced both the solubility—up to 40 000-fold compared to water—and the stability of curcumin. The eutectogel (both in the presence and absence of curcumin) possessed good antioxidant and anti-*P. acnes* activity. To sum up, the presented study provided a simple strategy for the development of a highly efficient carrier-free therapeutic eutectogel for treating *P. acnes* infection. Further clinical exploration of the proposed eutectogel is still ongoing.

Conflicts of interest

The authors declare no competing financial interests.

Data availability

All data generated or analyzed during this study are included in the published article.

Physical properties, *i.e.* density, viscosity, refractive index, surface tension, and viscosity of THEDES. See DOI: **https://doi.org/10.1039/d5ra03681j**.

Acknowledgements

The presented work was supported by the National Natural Science Foundation of China (No. 21773063), and Scientific Research Foundation of SUMHS (SSF-23-14-003).

References

1 T. Nakatsuji, M. C. Kao, J. Y. Fang, C. C. Zouboulis, L. F. Zhang, R. L. Gallo and C. M. Huang, Antimicrobial property of lauric acid against propionibacterium acnes: its therapeutic potential for inflammatory acne vulgaris, *J. Invest. Dermatol.*, 2009, **129**, 2480–2488.

2 W. C. Huang, T. H. Tsai, L. T. Chuang, Y. Y. Li, C. C. Zouboulis and P. J. Tsai, Anti-bacterial and anti-inflammatory properties of capric acid against Propionibacterium acnes: a comparative study with lauric acid, *J. Dermatol. Sci.*, 2014, **73**, 232.

3 D. Pornpattananangkul, V. Fu, S. Thamphiwatana, L. Zhang, M. Chen, J. Vecchio, W. W. Gao, C. M. Huang and L. F. Zhang, In vivo treatment of propionibacterium acnes infection with liposomal lauric acids, *Adv. Healthcare Mater.*, 2013, **2**, 1322–1328.

4 D. Yang, D. Pornpattananangkul, T. Nakatsuji, M. Chan, D. Carson, C. M. Huang and L. Zhang, The antimicrobial activity of liposomal lauric acids against Propionibacterium acnes, *Biomaterials*, 2009, **30**, 6035–6040.

5 T. Q. M. Tran, M. F. Hsieh, K. L. Chang, Q. H. Pho, V. C. Nguyen, C. Y. Cheng and C. M. Huang, Bactericidal effect of lauric acid-loaded PCL-PEG-PCL nano-sized micelles on skin, *Polymers*, 2016, **8**, 321.

6 M. A. R. Martins, S. P. Pinho and J. A. P. Coutinho, Insights into the nature of eutectic and deep eutectic mixtures, *J. Solution Chem.*, 2019, **48**, 962–982.

7 B. B. Hansen, S. Spittle, B. Chen, D. Poe, Y. Zhang, J. M. Klein, A. Horton, L. Adhikari, T. Zelovich, B. W. Doherty, B. Gurkan, E. J. Maginn, A. Ragauskas, M. Dadmun, T. A. Zawodzinski, G. A. Baker, M. E. Tuckerman, R. F. Savinell and J. R. Sangoro, Deep eutectic solvents: a review of fundamentals and applications, *Chem. Rev.*, 2021, **12**, 1232–1285.

8 H. Vanda, Y. T. Dai, E. G. Wilson, R. Verpoorte and Y. H. Choi, Green solvents from ionic liquids and deep eutectic solvents to natural deep eutectic solvents, *C. R. Chim.*, 2018, **21**, 628–638.

9 F. M. Perna, P. Vitale and V. Capriati, Deep eutectic solvents and their applications as green solvents, *Curr. Opin. Green Sustainable Chem.*, 2020, **21**, 27–33.

10 A. P. Abbott, E. I. Ahmed, K. Prasad, I. B. Qader and K. S. Ryder, Liquid pharmaceuticals formulation by eutectic formation, *Fluid Phase Equilib.*, 2017, **448**, 2–8.

11 Md S. Rahman, R. Roy, B. Jadhav, Md N. Hossain, M. A. Halim and D. E. Raynie, Formation, structure, and applications of therapeutic and amino acid-based deep eutectic solvents: an overview, *J. Mol. Liq.*, 2021, **321**, 114745.

12 M. M. Abdelquader, S. Li, G. P. Andrews and D. S. Jones, Therapeutic deep eutectic solvents: a comprehensive review of their thermodynamics, microstructure and drug delivery applications, *Eur. J. Pharm. Biopharm.*, 2023, **186**, 85–104.

13 J. M. Silva, C. V. Pereira, F. Mano, E. Silva, V. I. B. Castro, I. Sá-Nogueira, R. L. Reis, A. Paiva, A. A. Matias and A. R. C. Duarte, Therapeutic role of deep eutectic solvents based on menthol and saturated fatty acid on wound healing, *ACS Appl. Bio. Mater.*, 2019, **2**, 4346–4355.

14 J. M. Silva, E. Silva, R. L. Reis, A. Rita and A. R. C. Duarte, A closer look in the antimicrobial properties of deep eutectic solvents based on fatty acids, *Sustainable Chem. Pharm.*, 2019, **14**, 100192.

15 A. B. Kunnumakkara, M. Hegde, D. Parama, S. Girisa, A. Kumar, U. D. Daimary, P. Garodia, S. C. Yenisetti and O. V. Oommen, Role of Turmeric and Curcumin in Prevention and Treatment of Chronic Diseases: Lessons Learned from Clinical Trials, *ACS Pharmacol. Transl. Sci.*, 2023, **6**, 447–518.

16 T. Waghule, S. Gorantla, V. K. Rapalli, P. Shah, S. K. Dubey, R. N. Saha and G. Singhvi, Emerging trends in topical delivery of curcumin through lipid nanocarriers: effectiveness in skin disorders, *AAPS PharmSciTech*, 2020, **21**, 284.

17 C. H. Liu and H. Y. Huang, In vitro anti-propionibacterium activity by curcumin containing vesicle system, *Chem. Pharm. Bull.*, 2013, **61**, 419–425.

18 X. Lan, J. N. Zhao, Y. Zhang, Y. Chen, Y. Liu and F. Q. Xu, Oxymatrine exerts organ- and tissue-protective effects by regulating inflammation, oxidative stress, apoptosis, and fibrosis: From bench to bedside, *Pharmacol. Res.*, 2020, **151**, 104541.

19 D. Q. Huan, N. Q. Hop and N. T. Son, Oxymatrine: a current overview of its health benefits, *Fitoterapia*, 2023, **168**, 105565.

20 B. Li, T. Xiao, S. Guo, Y. Wu, R. Lai, Z. Liu, W. Luo and Y. Xu, Oxymatrine-fatty acid deep eutectic solvents as novel penetration enhancers for transdermal drug delivery: formation mechanism and enhancing effect, *Int. J. Pharm.*, 2023, **637**, 122880.

21 J. Y. Wu and T. X. Yin, Amphiphilic deep eutectic solvent based on lidocaine and lauric acid: formation of microemulsion and gel, *Langmuir*, 2022, **38**, 1170–1177.

22 Q. H. Yang, Z. N. Liu, T. X. Yin, X. Y. Wang and J. Yuan, Eutectogel based on multi-functional deep eutectic solvent for acne infection treatment, *J. Drug Delivery Sci. Technol.*, 2024, **101**, 106260.

23 M. H. Li, J. Yuan, Q. H. Yang, Z. N. Liu, S. X. Meng, X. Y. Wang, C. J. Peng and T. X. Yin, Therapeutic deep eutectic solvents based on natural product matrine and caprylic acid: physical properties, cytotoxicity and formation of surfactant free microemulsion, *J. Drug Delivery Sci. Technol.*, 2023, **90**, 105177.

24 P. R. Li, X. Wang, Y. L. Chen, T. X. Yin and W. G. Shen, Thermodynamic properties and structure transition in {water + tert-butanol} and {water + tert-butanol + iso-butanol} solutions, *Thermochim. Acta*, 2020, **686**, 178548.

25 J. Y. Wu and T. X. Yin, Novel paeonol-matrine deep eutectic solvent: Physicochemical properties and cytotoxicity, *J. Mol. Liq.*, 2022, **348**, 118068.
26 H. C. Andersen, Molecular dynamics simulations at constant pressure and/or temperature, *J. Chem. Phys.*, 1980, **72**(4), 2384–2393.
27 H. J. C. Berendsen, J. P. M. Postma, W. F. Van Gunsteren, A. DiNola and J. R. Haak, Molecular Dynamics with Coupling to an External Bath, *J. Chem. Phys.*, 1984, **81**(8), 3684–3690.
28 G. M. Yuvrajsinh, P. Rajput, G. V. Yuvrajsinh, S. Sharma, K. Singh, S. Adhikari and A. Kmar, Physicochemical and derived properties of novel phenol based deep eutectic solvents in the temperature range of 293.15-343.15K, *J. Mol. Liq.*, 2025, **424**, 127070.
29 K. Singh, R. P. Shibu, S. Mehra and A. Kumar, Insights into the physicochemical properties of newly synthesized benzyl triethylammonium chloride-based deep eutectic solvents, *J. Mol. Liq.*, 2023, **386**, 122589.
30 H. A. Papazian, Correlation of surface tension between various liquids, *J. Am. Chem. Soc.*, 1971, **93**, 5634–5636.
31 A. H. Pelofsky, Surface tension-viscosity relation for liquids, *J. Chem. Eng. Data*, 1966, **11**, 394–397.
32 M. H. Zainal-Abidin, M. Hayyan, G. C. Ngoh, W. F. Wong and C. Y. Looi, Emerging frontiers of deep eutectic solvents in drug discovery and drug delivery systems, *J. Controlled Release*, 2019, **316**, 168–195.
33 W. D. Lu and H. Q. Chen, Application of deep eutectic solvents (DESs) as trace level drug extractants and drug solubility enhancers: state-of-art, prospects and challenges, *J. Mol. Liq.*, 2022, **349**, 118105.
34 A. Sharma, Y. R. Park, A. Garg and B. S. Lee, Deep eutectic solvents enhancing drug solubility and its delivery, *J. Med. Chem.*, 2024, **67**, 14807–14819.
35 S. Kalantri and A. Vora, Eutectic solutions for healing: a comprehensive review on therapetic deep eutectic solvents (THEDES), *Drug Dev. Ind. Pharm.*, 2024, **50**, 387–400.
36 B. T. Kurien, A. Singh, H. Matsumoto and R. H. Scofield, Improving the solubility and pharmacological efficacy of curcumin by heat treatment, *Assay Drug Dev. Technol.*, 2007, **5**, 567–576.
37 J. Cao, J. R. Cao, H. M. Wang, L. Y. Chen, F. L. Cao and E. Z. Su, Solubility improvement of phytochemicals using (natural) deep eutectic solvents and their bioactivity evaluation, *J. Mol. Liq.*, 2020, **318**, 113997.
38 T. Jeliński, M. Przybyłek and P. Cysewski, Natural deep eutectic solvents as agents for improving solubility, stability and delivery of curcumin, *Pharm. Res.*, 2019, **36**, 116.
39 X. W. Du, J. Zhou, J. F. Shi and B. Xu, Supramolecular hydrogelators and hydrogels: from soft matter to molecular biomaterials, *Chem. Rev.*, 2015, **115**, 13165–13307.
40 B. O. Okesola and D. K. Smith, Applying low-molecular weight supramolecular gelators in an environmental setting-self-assembled gels as smart materials for pollutant removal, *Chem. Soc. Rev.*, 2016, **45**, 4226–4251.
41 S. Marullo, A. Meli, F. Giannici and F. D'Anna, Supramolecular eutecto gels: fully natural soft materials, *ACS Sustainable Chem. Eng.*, 2018, **6**, 12598–12602.
42 F. Delbecq, P. Delfosse, G. Laboureix, C. Pare and T. Kawai, Study of a gelated deep eutectic solvent metal salt solution as template for the production of size-controlled small noble metal nanoparticles, *Colloids Surf., A*, 2019, **567**, 55–62.
43 J. Ruiz-Olles, P. Slavik, N. K. Whitelaw and D. K. Smith, Self-assembled gels formed in deep eutectic solvents: supramolecular eutectogels with high ionic conductivity, *Angew. Chem., Int. Ed.*, 2019, **58**, 4173–4178.
44 C. Florindo, L. G. Celia-Silva, L. F. G. Martins, L. C. Branco and I. M. Marrucho, Supramolecular hydrogel based on a sodium deep eutectic solvent, *Chem. Commun.*, 2018, **54**, 7527–7530.